J. Chem. Thermodynamics 151 (2020) 106163

Contents lists available at ScienceDirect

J. Chem. Thermodynamics

journal homepage: www.elsevier.com/locate/jct

# Infinite dilution activity coefficients and thermodynamic properties of selected organic solutes and water dissolved in 1, 6-hexanediol

Nkululeko Nkosi [a], Kaniki Tumba [a,*], Peterson Ngema [b], Suresh Ramsuroop [b]

[a] Department of Chemical Engineering, Mangosuthu University of Technology, uMlazi, Durban 4031, South Africa
[b] Department of Chemical Engineering, Durban University of Technology, Steve Biko Campus, Durban 4001, South Africa

ARTICLE INFO

*Article history:*
Received 30 December 2019
Received in revised form 1 March 2020
Accepted 1 May 2020
Available online 5 May 2020

*Keywords:*
1.6-Hexanediol (HDO)
Activity coefficient at infinite dilution
Gas-to-liquid partition coefficient
Gas-liquid chromatography
Separation
Thermodynamic properties

ABSTRACT

The experimental activity coefficients ($\gamma_{13}^{\infty}$) and gas-to-liquid partition coefficients ($K_L$) at infinite dilution for 34 organic solutes and water were determined in 1.6-hexanediol (HDO) by the gas–liquid chromatography technique (GLC) in the temperature range from (323.15 to 353.15) K. Fundamental thermodynamic functions such as excess partial molar enthalpy ($\Delta H_i^{E,(\infty)}$), excess partial molar Gibbs energy, ($\Delta G_i^{E,\infty}$) and entropy, ($T_{ref}\Delta S_i^{E,\infty}$) at infinite dilution were calculated from experimental values of $\gamma_{13}^{\infty}$. Reported data were discussed in terms of solvent-solute interactions, heat effects and mixing spontaneity. Selectivity ($S_{ij}^{\infty}$) and capacity ($k_j^{\infty}$) related to different separation problems were calculated from $\gamma_{13}^{\infty}$ data and compared to the literature values for selected ionic liquids (ILs), deep eutectic solvents (DESs) and industrial solvents. New data reported in this study suggest that HDO may be proposed as an alternative solvent for the separation of alkanes-pyridine and alkanes-thiophene systems. Furthermore, it was found that adding a hydrogen bond acceptor to HDO enhances its performance as a separation solvent.



## 1. Introduction

1,6-Hexanediol (HDO), a linear diol with two primary hydroxyl groups is generally synthesised by catalytic hydrogenation of adipic acid or their esters [1–3]. Until now, as reaction media, HDO is commercially available with an estimated global production of approximately 138,000 tons $yr^{-1}$ [4]. It is a valuable speciality chemical that is industrially used for the manufacturing of polyesters, elastomers, acrylates, adhesives, coating materials, as well as polymeric plasticisers [5]. The use of HDO has also been extensively investigated in catalysis and extraction processes [6–11]. This solvent possesses interesting properties such as low flammability, good thermal stability and low toxicity. These properties and its availability make HDO a good candidate amongst prospective green separation solvents in replacement of less environmentally friendly solvents currently used in industry.

There are four different articles that stand out in the literature as good illustrations of the ability of HDO-based deep eutectic solvent to act as separation solvents. In deep eutectic solvents, HDO is used as hydrogen-bond donor (HBD). Park and co-researchers [12] reported the use of $ZnCl_2$ + 1,6-hexanediol (1:2) as an extractant for chlorogenic acid and caffeic acid from *Herba Artemisiae Scopariae*, a traditional medicine used for liver protection, blood pressure lowering, antipyretic as well as anti-inflammatory, antibacterial, antimicrobial, and antitumor activities. This hexanediol-based DES was ranked 7th out of 12 different DESs examined for their extraction ability. Yoo and co-workers [13] successfully used 1,6-hexanediol + choline chloride (7:1) in conjunction with ultrasound-assisted extraction to separate natural bioactive phenolics from spent coffee grounds. The reported yield was 92.3%, indicating that the investigated DES could be used to valorise spent coffee grounds. In another investigation, Cui and co-authors [14] successfully extracted bioactive compounds (genistin, genistein and apigenin) from pigeo pea roots. The hexanediol-based DESs (1.6-hexanediol + choline chloride) amongst others, was used as an extractant in a range of different molar ratios (1:1 to 8:1) and water content (0 to 90%) in DESs. These authors achieved an optimum extraction of bioactive compounds when a molar ratio and water content were 8:1 and 30%, respectively. This indicated its ability to be used in genistin, genistein and apigenin extraction from pigeon pea roots. In relation to separation processes relevant to Chemical Process Industries, Nkosi and co-workers investigated the potential use of two different HDO-based deep eutectic solvents, viz. tetramethylammonium chloride + 1, 6-hexanediol (1:1), [15] and tetrapropylammonium bromide + 1,6-hexanediol (1:2), [16]. It was found that hexanediol-based DESs have good potential to be used in fuel denitrification and desulfurisation processes.

* Corresponding author.
*E-mail address:* tumba@mut.ac.za (K. Tumba).

https://doi.org/10.1016/j.jct.2020.106163
0021-9614/

The aforementioned studies were prompted by safety and environmental concerns while searching for "green" alternative solvents to volatile organic compounds (VOCs). These solvents exhibit properties that are known to be toxic and harmful to humans as well as the environment. Along with ionic liquids (ILs), deep eutectic solvents (DESs) have been investigated as green replacements for volatile organic compounds (VOCs). It was reported that some ILs and DESs are likely to perform better than the currently used industrial solvents in numerous separation problems, on the basis of limiting activity coefficient data [15,16]. DESs continue to be regularly projected as green extractive solvents [17–22]. The screening of potential candidates as solvents for extraction processes can be achieved by experimental determination of activity coefficients at infinite dilution ($\gamma_{13}^{\infty}$). Limiting activity coefficient data give insights into the nature of intermolecular interactions between the solvent and the solute. Hence, they reflect the extent of solubility. Limiting activity coefficients allow calculation of extraction parameters, selectivity ($S_{ij}^{\infty}$) and capacity ($k_j^{\infty}$) at infinite dilution. Information associated with limiting activities can be used in the design of solvent-enhanced separation processes. Amongst various experimental methods, the steady-state gas–liquid chromatography (GLC) emerges as the most popular, expedient, cost-effective, and reliable technique to determine $\gamma_{13}^{\infty}$ in high-boiling solvents [23–25].

This study is concerned with the investigation of HDO as an extractant for various separation problems of industrial importance. Recently, our group investigated activity coefficients at infinite dilution of various organic solutes in two different DESs containing HDO [15,16]. These DESs revealed promising $S_{ij}^{\infty}$ and $k_j^{\infty}$ values and could be effective separation agents for alkanes-heterocyclics (thiophene and pyridine) and cycloalkanes or ketones or aromatics-alcohols, mixtures. However, our reported experimental data did not give any insight into the contribution of each component of the DESs towards its performance in denitrification and desulfurisation processes. It is against this background that the present investigation was initiated.

In this study, we report experimental infinite dilution activity coefficients and gas-to-liquid partition coefficients ($K_L$) for water and a set of 34 selected organic solutes – n-alkanes, alk-1-enes, cycloalkanes, alk-1-ynes, alkylbenzenes, ketones, alkanols, esters, heterocyclics and acetonitrile – in HDO. Limiting activity coefficients were determined by gas–liquid chromatography (GLC) in the temperature range from 323.15 K to 353.15 K. Experimental $\gamma_{13}^{\infty}$data were further used to determine basic thermodynamic functions such as excess partial molar enthalpy ($\Delta H_i^{E,(\infty)}$), Gibbs energy, ($\Delta G_i^{E,\infty}$) and entropy, ($T_{ref}\Delta S_i^{E,\infty}$), at infinite dilution. The obtained thermodynamics properties were examined in terms of intermolecular interactions to assess the possible use of HDO as separation solvent in liquid-liquid extraction as well as extractive distillation.

It is worth noting that Alessi and co-workers [26] undertook similar measurements and reported experimental data for a few organic solutes in HDO. In the current study, additional organic solutes were investigated (some new data are reported). Furthermore, additional thermodynamic properties were examined and comparison was made between HDO and some DESs, ILs as well popular industrial solvents (i.e. *N*-methyl-2-pyrrolidone and sulfolane).

## 2. Experimental

### 2.1. Materials

All solutes were used without further purification since the GLC technique separated any impurities on the column. The list of solutes, including sources and stated purities, are presented in Table 1S as part of Supplementary Materials. HDO was degassed and dried for 24 h at $T$ = 313.15 K under vacuum to reduce water content and volatile impurities. The structure of HDO is shown in Fig. 1. The solid support material (Chromosorb W-HP 80/100 mesh) was dried by vacuum purification at $T$ = 363.15 K for 6 h to remove any absorbed moisture prior to its use as adsorbent. It was supplied by Supelco (USA) while dichloromethane served as dispersion promoter solvent. The GC carrier gas was helium.

### 2.2. Experimental procedures

#### 2.2.1. Density, and refractive index and viscosity measurements

In this study, densities, viscosities and refractive indices of HDO were measured at atmospheric pressure in the temperature ranges from (313.15 to 353.15) K and (313.15 to 343.15) K, respectively. The detailed procedure was given in a previous study [17]. The measured properties are given in Table 1 where good agreement with literature data is observed.

*Density measurements.* Densities were measured using an Anton Paar density and sound velocity meter (model DSA 5000M, from Anton Paar USA Inc ) incorporating the vibrating U-tube technique. The instrument was equipped with a built-in Peltier thermostat that controlled and maintained temperature values within ±0.01 K. Two different fluids (millipore water and methanol) were used to calibrate this instrument following the detailed procedure provided in a previous study [17]. The validation and precision of the calibration procedure were confirmed by using NIST certified fluid standards data. In order to verify the reliability, reproducibility and accuracy of the measured densities for HDO, three readings were measured for each temperature, and the average value was finally reported. The uncertainty on density measurements at corresponding temperature was estimated as ±1.7 × $10^{-3}$ g.cm $^{-3}$.

*Refractive index*

Refractive index of HDO was measured using an Atago refractometer (model RX7000) with temperature control within ±0.05 K. The instrument was calibrated by measuring the refractive index of millipore water before each measurement. The calibration procedure was confirmed by using the known and certified refractive index of millipore water. The measurement uncertainty was ±1.4 × $10^{-3}$.

*Viscosity measurements*

Viscosity measurements were carried out using an Anton Paar AMVn rolling-ball viscometer T = (313.15, 323.15, 343.15 and 353.15) K at atmospheric pressure. The temperature was controlled internally using a built-in Peltier thermostat with a precision of ±0.01 K. Before the experiment, the viscometer's reliability was confirmed by measuring the viscosity of the standards provided by the supplier. There was a good agreement between the values obtained in this study and those provided by the supplier for the standard. The apparatus and the experimental technique used in this study for the measurement of HDO viscosity were described in the l iterature [27]. Viscosity values were determined using the following equation (1), [30]:

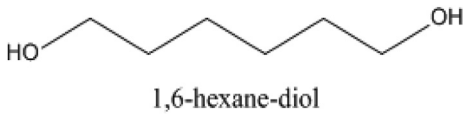


1,6-hexane-diol

**Fig. 1.** The structure of the investigated solvent, 1,6 hexanediol (hexamethylene glycol).

**Table 1**
Properties of the investigated solvent (1,6 hexanediol): experimental density ($\rho$), refractive index ($RI$) and viscosity ($\mu$) at $T$ = (313.15, 323.15, 333.15, 343.15 and 353.15) K and at $p$ = (101.3 ± 2) kPa; 1,6 hexanediol was in liquid state.

| $T$/K | $\rho$/g.cm$^{-3}$ | | | $\mu$ /mPa.s | | | | | $R/I$ |
|---|---|---|---|---|---|---|---|---|---|
| | Exp | Lit.[a,*] | %ARD | Exp | Lit.[a,*] | %ARD[a] | Lit.[b,*] | %ARD[b] | Exp |
| 313.15 | 0.9591 | – | – | 59.111 | – | – | 60.203 | 1.81 | 1.4470 |
| 323.15 | 0.9532 | 0.9549 | 0.18 | 38.427 | 40.465 | 5.03 | 38.596 | 0.44 | 1.4441 |
| 333.15 | 0.9473 | 0.9488 | 0.16 | 25.789 | 27.141 | 4.95 | 25.994 | 0.75 | 1.4412 |
| 343.15 | 0.9413 | 0.9426 | 0.13 | 18.039 | 17.755 | 1.6 | 17.901 | 0.77 | 1.4379 |
| 353.15 | – | 0.9364 | – | 13.024 | 12.876 | 1.15 | 12.186 | 6.88 | – |

Standard uncertainties: $u(T)$ = 0.01 K and 0.05 K for density and refractive index, respectively, and $u(\rho)$ = 1.7 × 10$^{-3}$ g·cm$^{-3}$, $u(p)$ = 2 kPa, $u(RI)$ = 1.4 × 10$^{-3}$, $u(\mu)$ = 4.43% of measured values.
[*] Interpolated.
[a] Ref. [31].
[b] Ref. [32].

$$\mu = t_o\, k_\alpha\, [\rho_{ball} - \rho_{HDO}] \quad (1)$$

where μ is the HDO viscosity, $k_\alpha$ the calibration constant of the viscometer, $t_0$ is the average time taken by the ball to fall, ρball is the density of the rolling ball and $\rho_{HDO}$ is the density of HDO at T. The solvent shear stress was selected by setting a nominal capillary angle of inclination to 50° with the horizontal plane. The experimental recorded averaged rolling times for HDO were less than 200 s with a precision of ± 0.002 s. As a result, the diameters of the nominal capillary (1.8 mm) and the ball (1.5 mm) for the measured HDO viscosity range (2.5 to 70 mPa.s) were selected. The experimental dynamic viscosities of HDO are listed in Table 1 as well.

*2.2.2. Water content*

Karl-Fischer moisture titrator (870 KF Titrino Plus) was used to analyse the water content in the HDO sample before preparing the column. HDO was dissolved in methanol and titrated in steps of 0.009 mL. HDO water content was 0.0001 mol fraction (Uncertainty: ± 0.00005)

*2.2.3. Activity coefficient measurements*

The experimental procedure used for the measurement of activity coefficients at infinite dilution ($\gamma_{13}^{\infty}$) in HDO has been described in detail in previous publications [15–17,30]. It is only briefly explained here. A Shimadzu 2014 gas chromatograph equipped with a thermal conductivity (TCD) and a flame ionisation (FID) detectors as well as a heated on-column injector was used in this study. The injector and detector temperatures were fixed at 523.15 K for the duration of all experimental measurements. The column dead time, $t_G$, was determined using air as the unretained solute. The helium (carrier gas) flow rate was measured with a bubble soap flow meter fitted to the TCD vent line.

The preparation of the column was described in our previous studies [15–17,30]. Packed columns of 0.5 m length containing two different solvent loadings with an estimated uncertainty of 2 × 10$^{-4}$ mmol, namely (0.2725 and 0.3305) wt fraction were prepared to monitor adsorption effects. The stationary phase (HDO) coated onto a solid support material (Chromosorb W-HP 80/100 mesh) was prepared by allowing IL to dissolve in dichloromethane and dispersed in Chromosorb. Briefly, HDO was dissolved in dichloromethane in the presence of a precise mass (±0.0001 g) of the solid support. The rest of the dichloromethane was continually evaporated from the mixture using a vacuum pump at 60 kPa. The conditioning of the packed columns was performed at 363.15 K for more than 8 h at a gas flow rate of 15 mL.min$^{-1}$. It is estimated that the uncertainty was 0.15 mL·min$^{-1}$. The mass of the packed columns was checked periodically during the experimental measurements. A typical injection ranged from (0.1 to 0.2) $\mu L$ to comply with the requirement for the "infinite dilution" region. A minimum of three injections was used for each data point to ensure that the measured values were reproducible. It was determined that measured retention times were reproducible within ($10^{-3}$ to $10^{-2}$) min depending upon the column temperature and the individual solute.

Overall uncertainties of $\gamma_{13}^{\infty}$, $K_L$, $\Delta G_i^{E,\infty}$, $\Delta H_i^{E,(\infty)}$ and $T_{ref}\Delta S_i^{E,\infty}$ were found by taking into account the possible uncertainties in determining the retention times, solute vapour pressure and column loading using the calculation procedure described by Bahadur and co-researchers [31].

## 3. Theory

In this study, experimental activity coefficients at infinite dilution ($\gamma_{13}^{\infty}$) for solutes (1) in a non-volatile solvent, HDO were obtained from solute retention times according to the Eq. (2) developed by Everett [32] and Cruickshank et al. [33]:

$$\ln\gamma_{13}^{\infty} = \ln\left(\frac{n_3 RT}{V_N P_{*1}}\right) - \frac{(B_{11} - v_{*1})P_{*1}}{RT} + \frac{(2B_{12} - v_1^{\infty})J_2^3 P_o}{RT} \quad (2)$$

where $n_3$ is the number of moles of solvent in the column packing; R is the gas constant; $V_N$ denote the net retention volume; $P_o$ is the column outlet pressure and is the same as the atmospheric pressure; $P_{*1}$ is the saturated vapour pressure of the solute (1) at temperature $T$, obtained through Antoine Equation [34];$B_{11}$ is the second virial coefficient of the pure solutes (1); $B_{12}$ is the mixed second virial coefficient of the solute (1) and carrier gas (2); and$J_2^3 P_o$ is the mean column pressure; $v_{*1}$ is the molar volume of the solute, and $v_1^{\infty}$ is the partial molar volume of the solute (1) at infinite dilution (expressed as the molar volume of the solute) in the solvent.

The parameters used to determine activity coefficients at infinite dilution were obtained from various thermodynamics tables, given by [34] and [35]. Both $B_{11}$ and $B_{12}$ were determined using the Equation detailed by [36]:

$$B/V_c = 0.43 - 0.886\left(\frac{T_c}{T}\right) - 0.694\left(\frac{T_c}{T}\right)^2 - 0.0375\,(n-1)\left(\frac{T_c}{T}\right)^{4.5} \quad (3)$$

where $n$ denotes the number of carbon atoms in the solute molecule. The mixing rules of [37] were used to determine the values of mixed properties from the critical properties ($T_{c12}$, $V_{c12}$ and ionisation energy) of the pure components. The virial coefficients of the alcohols and ketones were calculated using correlations by Tsonopoulos [38]. The pressure correction term detailed by is given by [32]:

$$J_2^3 = \left(\frac{2}{3}\right)\left[\frac{\left(\frac{P_i}{P_o}\right)^3 - 1}{\left(\frac{P_i}{P_o}\right)^2 - 1}\right] \quad (4)$$

**Table 2**
Activity coefficients at infinite dilution for selected organic solutes (1) in 1,6 hexanediol (3) at T = (323.15, 333.15, 343.15, and 353.15) K. The standard state for solutes is hypothetical liquid at zero pressure.

| Solute | *T*/K | | | |
|---|---|---|---|---|
| | 323.15 | 333.15 | 343.15 | 353.15 |
| n-pentane | 15.722 | 14.076 | 12.278 | 11.379 |
| n-hexane | 21.713 | 19.665 | 18.209 | 16.754 |
| n-heptane | 29.730 | 27.963 | 26.040 | 23.700 |
| n-octane | 39.381 | 37.141 | 35.128 | 32.442 |
| n-nonane | 52.651 | 49.473 | 46.592 | 43.720 |
| cyclopentane | 9.351 | 8.720 | 8.110 | 7.661 |
| cyclohexane | 13.372 | 12.424 | 11.672 | 11.119 |
| cyloheptane | 15.765 | 14.903 | 14.407 | 13.789 |
| cyclooctane | 19.098 | 17.985 | 17.157 | 16.261 |
| hex-1-ene | 15.411 | 14.066 | 12.869 | 11.637 |
| hept-1-ene | 21.731 | 20.402 | 18.857 | 17.614 |
| hex-1-yne | 9.109 | 8.407 | 8.014 | 7.641 |
| hept-1-yne | 10.846 | 10.524 | 10.112 | 9.938 |
| oct-1-yne | 14.828 | 14.414 | 14.052 | 13.601 |
| methanol | 0.902 | 0.879 | 0.863 | 0.848 |
| ethanol | 1.055 | 1.036 | 1.019 | 1.008 |
| propan-1-ol | 1.198 | 1.178 | 1.167 | 1.152 |
| propan-2-ol | 1.151 | 1.148 | 1.146 | 1.143 |
| butan-1-ol | 1.393 | 1.387 | 1.377 | 1.372 |
| *tert*-butanol | 1.150 | 1.173 | 1.215 | 1.238 |
| benzene | 5.079 | 4.917 | 4.796 | 4.677 |
| toluene | 6.779 | 6.627 | 6.507 | 6.327 |
| ethylbenzene | 9.300 | 8.984 | 8.805 | 8.503 |
| *o*-xylene | 8.569 | 8.328 | 8.162 | 7.859 |
| *m*-xylene | 9.076 | 8.852 | 8.701 | 8.464 |
| *p*-xylene | 9.036 | 8.841 | 8.587 | 8.314 |
| acetone | 2.733 | 2.538 | 2.374 | 2.234 |
| butan-2-one | 3.215 | 3.012 | 2.877 | 2.697 |
| pentan-2-one | 3.901 | 3.706 | 3.538 | 3.346 |
| water | 1.505 | 1.513 | 1.519 | 1.534 |
| thiophene | 0.458 | 0.465 | 0.474 | 0.486 |
| pyridine | 0.082 | 0.087 | 0.092 | 0.097 |
| methyl acetate | 0.513 | 0.500 | 0.488 | 0.468 |
| ethyl acetate | 0.501 | 0.471 | 0.456 | 0.429 |
| acetonitrile | 3.996 | 3.626 | 3.345 | 3.052 |

Standard uncertainties: $u(T)$ = 0.05 K, and $u(\gamma_{13}^{\infty})$ = ± 5% of measured values.

The net retention volume of the solute (1) $V_N$, was determined using the Equation given by [25]:

$$V_N = \left(J_2^3\right)^{-1} U_o(t_R - t_G) \tag{5}$$

where $J_2^3$ denotes the pressure correlation term; $t_R$ and $t_G$ denotes the retention times for the solutes and the retention times for the un-retained gas and; $U_o$ is the column volumetric flow rate of the carrier gas that was measured with a soap bubble flow meter and corrected for the effects of water vapour pressure with the following Equation:

$$U_o = U\left(1 - \frac{P_w}{P_o}\right)\frac{T}{T_f} \tag{6}$$

where $T_f$ is the temperature of the flow meter; $P_w$ denotes the vapour pressure of water at $T_f$ and; $U$is the volumetric flow rate of the measured carrier gas by bubble flow meter at column outlet. The saturated vapour pressures for all solutes were calculated using the Antoine, modified Antoine or Wagner Equations in compliance with the applicability range of each correlation. Constants for the vapour pressure and correlations were obtained in the literature [35,36].

## 4. Results and discussion

### 4.1. Viscosity and density data

The measured physical properties (viscosity and density) of HDO were compared to those from literature [31,32]. Results obtained in this study were in good agreement with the most accurate available literature data. All relevant information regarding these data is contained in Table 1 and graphically shown in Figures S1 and S2 presenting the effect of temperature on the examined properties (See supplementary materials). As it can be seen, the agreement between experimental results and those reported in the literature was acceptable. Relative deviations for density were between 0.13 and 0.18 %, while they ranged from 1.15 to 6.88 % for viscosity. The decrease in density and viscosity was observed with increased temperature.

### 4.2. Activity coefficients at infinite dilution and other thermodynamic properties

Experimental activity coefficient at infinite dilution ($\gamma_{13}^{\infty}$) and gas-to-liquid partition coefficients ($K_L$) data of 34 organic solutes and water for the given solvent (HDO) are presented in Tables 2 and 3. Each reported value represents the corresponding average obtained from two different column loadings. The data published by Alessi and co-workers [26] were in good agreement with those reported in this article for various solutes, except for ethanol, methanol, methylacetate, ethylacetate and acetonitrile as shown in Table S3 of supplementary materials. Care was taken to observe that 1, 6 hexanediol was actually liquid at 313.15K, the lowest temperature considered in this study. (There are discrepancies in the literature regarding the actual melting pont of this solvent as some sources report a melting point of 315.15 K). Figs. 2–5 show plots obtained from experimental data provided in Table 2. They illustrate the temperature dependence of limiting activity coeffi-

**Table 3**
The experimental (gas–liquid) partition coefficients $K_L$ for the solutes and water (1) in 1,6-hexanediol (3) at $T$ = (323.15, 333.15 and 343.15) K and $p$ = (101.3 ± 2) kPa.

| Solute | T/K | | |
|---|---|---|---|
| | 323.15 | 333.15 | 343.15 |
| n-pentane | 1.065 | 0.772 | 0.632 |
| n-hexane | 1.734 | 1.448 | 1.179 |
| n-heptane | 3.227 | 2.725 | 2.050 |
| n-octane | 9.806 | 5.440 | 3.905 |
| n-nonane | 20.302 | 10.690 | 7.337 |
| cyclopentane | 2.752 | 1.771 | 1.393 |
| cyclohexane | 5.535 | 3.373 | 2.617 |
| cyloheptane | 9.015 | 5.871 | 4.481 |
| cyclooctane | 15.192 | 8.525 | 6.517 |
| hex-1-ene | 2.634 | 1.747 | 1.329 |
| hept-1-ene | 5.405 | 3.164 | 2.473 |
| hex-1-yne | 6.218 | 3.737 | 2.891 |
| hept-1-yne | 13.207 | 7.421 | 5.480 |
| oct-1-yne | 27.649 | 19.077 | 10.209 |
| methanol | 52.256 | 28.300 | 19.807 |
| ethanol | 84.336 | 43.453 | 29.160 |
| propan-1-ol | 180.206 | 88.238 | 56.359 |
| propan-2-ol | 95.275 | 47.726 | 31.136 |
| Butan-1-ol | 407.920 | 190.140 | 116.256 |
| *tert*-butanol | 96.149 | 47.200 | 29.772 |
| benzene | 14.224 | 8.343 | 6.267 |
| toluene | 31.258 | 17.263 | 5.658 |
| ethylbenzene | 59.485 | 31.686 | 21.884 |
| *o*-xylene | 88.981 | 46.355 | 31.476 |
| *m*-xylene | 68.582 | 35.876 | 24.483 |
| *p*-xylene | 66.108 | 34.688 | 23.837 |
| acetone | 7.603 | 7.333 | 5.890 |
| butan-2-one | 22.921 | 13.674 | 10.388 |
| pentan-2-one | 42.891 | 24.302 | 17.874 |
| water | 138.290 | 70.571 | 46.102 |
| thiophene | 20.724 | 11.870 | 8.831 |
| pyridine | 348.367 | 177.874 | 118.413 |
| methyl acetate | 8.169 | 5.090 | 4.083 |
| ethyl acetate | 14.321 | 8.573 | 6.548 |
| acetonitrile | 19.280 | 11.945 | 9.400 |

Standard uncertainties: $u(T)$ = 0.02 K, and $u(K_L)$ = ± 4% of measured values.

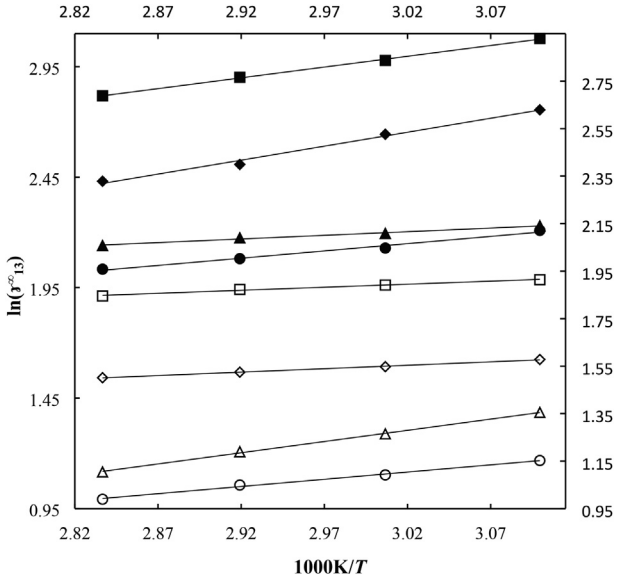


**Fig. 2.** Plot of ln ($\gamma_{13}^{\infty}$) against 1/T at $p$ = (101.3 ± 2) kPa for n-pentane (◆); n-hexane (■); ethylbenzene (▲); hex-1-yne (●); toluene (□); benzene (◇); acetonitrile (△); butan-2-one (○) (1) in 1.6-hexanediol (3).

cients for the investigated solutes in HDO. From Table 2, it can be seen that $\gamma_{13}^{\infty}$values for alkanes, alk-1-enes, alk-1-ynes, cycloalkanes, alkanols, alkylbenzenes, ketones, and esters were decreasing

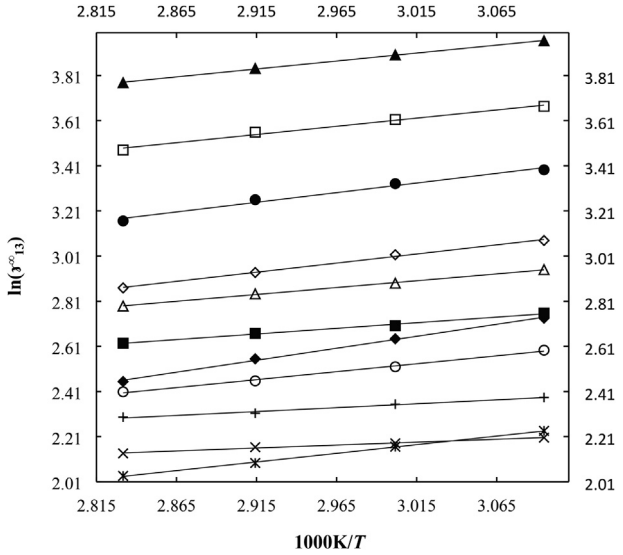


**Fig. 3.** Plot of ln ($\gamma_{13}^{\infty}$) against 1/T at $p$ = (101.3 ± 2) kPa for hex-1-ene (◆); cycloheptane (■); n-nonane (▲); n-heptane (●); n-octane (□); hep-1-ene (◇); cyclooctane (△); cyclohexane (○); hept-1-yne (+); *m*-xylene (×); cyclopentane (*) (1) in 1.6-hexanediol (3).

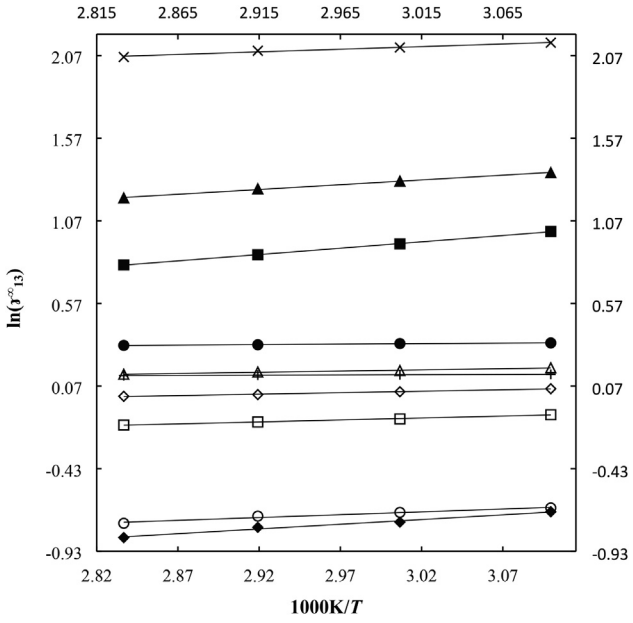


**Fig. 4.** Plot of ln ($\gamma_{13}^{\infty}$) against 1/T at $p$ = (101.3 ± 2) kPa for ethylacetate (◆); acetone (■); pentan-2-one (▲); butan-1-ol (●); methanol (□); ethanol (◇); propan-1-ol (△); methylacetate (○); propan-2-ol (+); *o*-xylene (×) (1) in 1.6-hexanediol (3).

with increasing temperature. The opposite trend was observed for heterocyclics compounds, i.e. pyridine and thiophene. The observed gentle slopes indicate weak dependence on temperature. The highest values of $\gamma_{13}^{\infty}$ were observed at all temperatures for n-nonane; $\gamma_{13}^{\infty}$= 52.651 at 323.15 K. The lowest values of activity coefficient were obtained for heterocyclics, i.e. pyridine ($\gamma_{13}^{\infty}$ = 0.082) and thiophene ($\gamma_{13}^{\infty}$ = 0.458) at 323.15 K. Fig. 6 indicates the effect of molecular structure and alkyl carbon chain length on $\gamma_{13}^{\infty}$ values. It was observed that limiting activity coefficients decreased in the following order: n-alkanes > alk-1-enes > cycloalkanes > alk-1-ynes > alkylbenzenes > ketones > alkanols > esters > heterocyclics. Measurements of $\gamma_{13}^{\infty}$ of thiophene and pyridine in hexanediol resulted in values lower than one in the entire range of tempera-

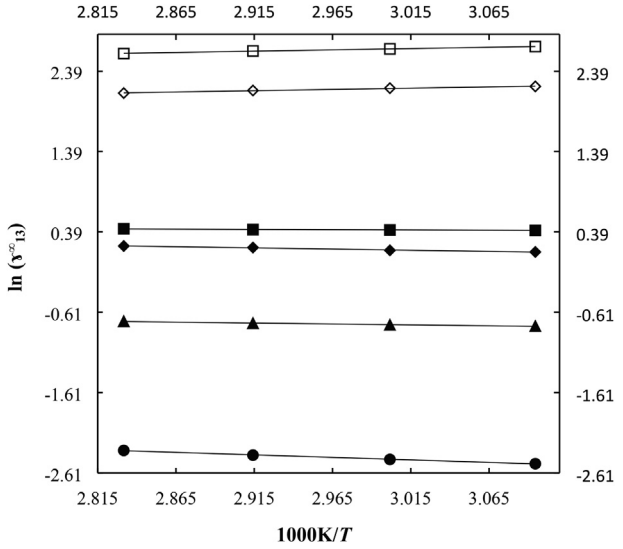


**Fig. 5.** Plot of ln ($\gamma_{13}^{\infty}$) against 1/T $p$ = (101.3 ± 2) kPa for *tert*-butanol (◆); water (■); thiophene (▲); pyridine (●); oct-1-yne (□); *p*-xylene (◇) in 1.6-hexanediol (3).

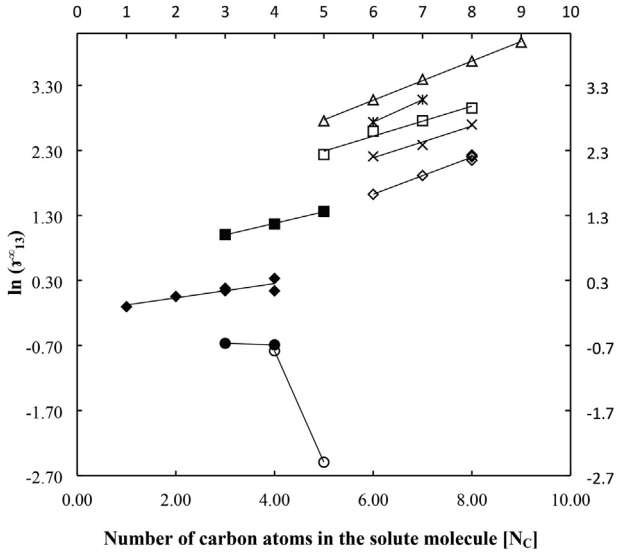


**Fig. 6.** Plot of ln ($\gamma_{13}^{\infty}$) against 1/T at $p$ = (101.3 ± 2) kPa for alkanols (◆); alkanes (△); alk-1-ynes (*), cycloalkanes (□), alk-1-ynes (×), alkylbenzenes (◇), heterocyclics (▲), ketones (■) and esters (●) in the 1.6-hexanediol at 323.15 K.

ture under investigation. This means that solvent-heterocyclic compound systems exhibited negative deviations from ideal behaviour.

As expected, polarity plays a notable role in the solubility behaviour of solutes in the investigated solvent, HDO which is polar in nature. Furthermore, it should be noted that low limiting activity coefficient values correspondent to strong solute-solvent interactions. Hence, from Fig. 6, it is observed that molecular interactions between solutes and the solvent decreased as alkyl chain length increased. The observed values indicated that non-polar compounds such as n-alkane, alk-1-enes, alk-1-ynes and cycloalkanes exhibited higher values of $\gamma_{13}^{\infty}$ compared to other solutes, which indicates weak attractive forces between these solute and HDO due to their low solubility. On the contrary, the possibility of strong dipole-dipole interactions between polar solutes and HDO explains low limiting activity coefficients obtained for ketones, alcohols, esters and hetrocyclic compounds. These polar compounds are therefore expected to be soluble in HDO as they were prone to be retained in the HDO stationary phase actively. The branching of hydrocarbons skeletons reduced the values of $\gamma_{13}^{\infty}$ in comparison with the corresponding linear n-alkanes. The presence of double or triple bonds within a solute molecule causes a reduction in activity coefficient values; thus, in this case, strong solute-solvent interactions occur due to the presence of delocalised π-electrons. In other words, these low limiting activity coefficient values for unsaturated hydrocarbons can be attributed to the presence of induced dipole-dipole interactions.

In this study, excess partial molar enthalpy ($\Delta H_i^{E,\infty}$), excess partial molar Gibbs free energy ($\Delta G_i^{E,\infty}$) and excess partial molar entropy ($T_{ref}\Delta S_i^{E,\infty}$) values at infinite dilution, for all examined solutes in HDO at the reference temperature of 323.15 K, were determined from reported$\gamma_{13}^{\infty}$. These thermodynamic functions provided further insight into the nature of solute-solvent molecular interactions.

The natural logarithm of limiting activity coefficient, ln $\gamma_{13}^{\infty}$ could be split into its respective $\Delta H_i^{E,\infty}$ and $T_{ref}\Delta S_i^{E,\infty}$ contributions:

$$\ln\gamma_{13} = \frac{\Delta H_i^{E,\infty}}{RT} - \frac{\Delta S_i^{E,\infty}}{R} \tag{7}$$

The two thermodynamic properties ($\Delta H_i^{E,\infty} = Ra$ and $\Delta S_i^{E,\infty} = -Rb$) were calculated by assuming van't Hoff relation, from its slope and intercept of the linear dependence on temperature as follows:

$$\ln\gamma_{13}^{\infty} = \frac{a}{T} + b \tag{8}$$

In the above equation, $a$ and $b$ represent the slope and intercept of the straight line. Excess partial molar Gibbs energies were calculated from the equation below [39]:

$$\Delta G_i^{E,\infty} = RT\ln\left(\gamma_{13}^{\infty}\right) = \Delta H_i^{E,\infty} - T_{ref}\Delta S_i^{E,\infty} \tag{9}$$

The results of the calculated values of the thermodynamics functions describing the temperature dependence for studied solutes in HDO are presented in Table 4. In this study, the limiting excess partial molar enthalpies, exhibit positive values for all solutes except for pyridine, thiophene, water and *tert*-butanol. The positive values of limiting excess molar enthalpy imply that dissociation effects outweighed the association effects in mixtures that involved the studied HDO and the investigated solutes under infinite dilution conditions. The negative $\Delta H_i^{E,\infty}$ values indicate the opposite effect and also denotes strong associative molecular interactions between the solutes and the solvent. Furthermore, positive $\Delta H_i^{E,\infty}$ values indicate that these solutes possess an endothermic (negative deviation from Raoult's law) heat of mixing when contacted with HDO. Negative $\Delta H_i^{E,\infty}$ values imply exothermic heats (positive deviation from Raoult's law) of mixing. $\Delta S_i^{E,\infty}$ occurred as both positive and negative and were decreasing with increasing alkyl chain length except for thiophene, pyridine, methyl acetate and ethyl acetate. The observed negative values of entropy indicate that adding solutes to HDO was accompanied by entropy losses. This suggests that solute molecules arranged an organised structure with HDO molecules. The limiting partial Gibbs energies for most studied solutes are positive. All solutes displaying negative limiting Gibbs energies were polar, except hex-1-ene. These polar molecules were small alcohols, small ketones, esters, and heterocyclic compounds. Negative excess molar Gibbs free energies indicate that mixing was spontaneous when these solutes were contacted with HDO. Unlike other unsaturated hydrocarbons, hex-1-ene + HDO mixtures appear to be characterised by very strong induced dipole – dipole interactions resulting in high solubility as suggested by its corresponding negative excess molar Gibbs free energy at infinite dilution.

**Table 4**
Limiting partial molar excess enthalpies ($\Delta H_i^{E,(\infty)}$), Gibbs free energies ($\Delta G_i^{E,\infty}$) and entropies ($T_{ref}\Delta S_i^{E,\infty}$) for organic solutes in 1,6 hexanediol at a reference temperature $T_{ref}$ = 323.15 K and $p$ = (101.3 ± 2) kPa.

| Solute | $a$ | $b$/K | $\Delta G_i^{E,\infty}$ /kJ·mol$^{-1}$ | $\Delta H_i^{E,(\infty)}$ /kJ·mol$^{-1}$ | $T_{ref}\Delta S_i^{E,\infty}$ /kJ·mol$^{-1}$ |
|---|---|---|---|---|---|
| n-pentane | 3.587 | 1264.61 | 0.878 | 10.514 | 9.636 |
| n-hexane | 0.020 | 976.06 | 8.570 | 8.115 | 0.055 |
| n-heptane | −2.341 | 854.82 | 13.397 | 7.107 | −6.29 |
| n-octane | 4.437 | 725.40 | 17.954 | 6.031 | −11.92 |
| n-nonane | −5.527 | 704.60 | 20.705 | 5.858 | −14.848 |
| cyclopentane | 0.415 | 999.04 | 7.190 | 8.306 | 1.116 |
| cyclohexane | −1.268 | 704.23 | 9.263 | 5.855 | −3.408 |
| cyloheptane | −3.758 | 497.72 | 14.235 | 4.138 | −10.097 |
| cyclooctane | −3.338 | 604.40 | 13.991 | 5.025 | −8.965 |
| hex-1-ene | 1.693 | 345.44 | −1.676 | 2.872 | 4.548 |
| hept-1-ene | −1.803 | 808.16 | 11.529 | 6.719 | −4.844 |
| Hex-1-yne | −0.512 | 657.93 | 6.846 | 5.470 | −1.376 |
| hept-1-yne | −4.065 | 345.44 | 13.800 | 2.872 | −10.928 |
| oct-1-yne | −5.245 | 324.15 | 16.786 | 2.695 | −14.091 |
| methanol | 2.557 | 233.10 | −4.930 | 1.938 | 6.869 |
| ethanol | 1.528 | 176.57 | −2.637 | 1.468 | 4.106 |
| propan-1-ol | 0.823 | 143.85 | −1.015 | 1.196 | 2.212 |
| propan-2-ol | −0.176 | 27.06 | 0.698 | 0.225 | −0.473 |
| Butan-1-ol | −0.457 | 59.54 | 1.722 | 0.495 | −1.227 |
| *tert*-butanol | −3.239 | −293.84 | 6.260 | −2.443 | −8.703 |
| benzene | −2.043 | 311.40 | 8.079 | 2.589 | −5.490 |
| toluene | −3.467 | 256.92 | 11.450 | 2.136 | −9.314 |
| ethylbenzene | 3.745 | 329.44 | 12.799 | 2.739 | −10.061 |
| *o*-xylene | −3.605 | 318.26 | 12.331 | 2.646 | −9.685 |
| *m*-xylene | −4.350 | 258.72 | 13.838 | 2.151 | −11.687 |
| *p*-xylene | −3.785 | 317.18 | 12.807 | 2.637 | −10.170 |
| acetone | 4.245 | 767.86 | −5.020 | 6.384 | 11.404 |
| butan-2-one | 2.639 | 652.86 | −1.661 | 5.428 | 7.089 |
| pentan-2-one | 1.313 | 577.58 | 1.275 | 4.802 | 3.527 |
| water | −1.934 | −70.12 | 4.614 | −0.583 | −5.197 |
| thiophene | 0.245 | −228.05 | −2.554 | −1.896 | 0.659 |
| pyridine | 1.730 | −626.53 | −9.857 | −5.209 | 4.648 |
| methyl acetate | 5.338 | 343.04 | −11.491 | 2.852 | 14.342 |
| ethyl acetate | 7.614 | 571.45 | −15.704 | 4.751 | 20.455 |
| acetonitrile | 5.433 | 1014.92 | −6.158 | 8.438 | 14.596 |

Standard uncerntainties $u$ are as follows: $u(T)$ = 0.05 K, $u(\Delta G_i^{E,\infty}, \Delta H_i^{E,(\infty)}, T_{ref}\Delta S_i^{E,\infty})$ = ± 8% of reported values.

Another important purpose of this study was to examine the potential use of HDO in selected solvent-enhanced industrial separation processes. This was achieved by calculating gas-to-liquid partition coefficient ($K_L$), selectivity ($S_{ij}^{\infty}$) and capacity ($k_j^{\infty}$) values at infinite dilution. The gas-to-liquid partition coefficient, $K_L = C^L/C^G$ for a solute (1) partitioning between a carrier gas (2) and a solvent (3) was calculated from solute retention data according to the following Eq. (10):

$$\ln K_L = \ln\left(\frac{V_N \rho_3}{m_3}\right) - \frac{P_o j_2^3 (2B_{12} - V_1^{\infty})}{RT} \tag{10}$$

where $\rho_3$ is the density of the solvent. The experimental $K_L$ data for various solutes between helium and HDO at different temperatures are presented in Table 3. It was found that $K_L$ values decreased with an increase of temperature in all solutes and increased with an increase in the alkyl chain length. The lowest $K_L$ values were observed for n-alkanes (at 343.15 K, for n-pentane, $K_L$ = 0.632), cycloalkanes, alk-1-enes and alk-1-ynes. The highest value was obtained for butan-1-ol at 323.15 K ($K_L$ = 407.92). High $K_L$ values correspond to large affinity of the solute with the liquid phase.

### 4.3. Evaluation of the performance of 1, 6-hexanediol in separation processes

The experimental data presented in Table 2 were used to assess HDO as separation agent in various separation problems. This was done by calculating $S_{ij}^{\infty}$ and $k_j^{\infty}$ as follows:

$$S_{ij}^{\infty} = \frac{\gamma_i^{\infty}}{\gamma_j^{\infty}} \tag{11}$$

$$k_j^{\infty} = \frac{1}{\gamma_j^{\infty}} \tag{12}$$

where $i$ refers to solutes and $j$ to the component to be extracted. The significance of Eqs. (11) and (12) is explained in the literature [41–43]. A comparison between HDO and other solvents such as ILs, DESs and popular industrial solvents (i.e. sulfolane and NMP) is presented at $T$ = 323.15 K in Table 5. $S_{ij}^{\infty}$ and $k_j^{\infty}$ values are made available for for heptane-hept-1-yne, heptane-thiophene, heptane-propan-2-none, water-butanol, cyclohexane-benzene, hexane-methanol, octane-acetonitrile, octane-ethyl acetate and ethylbenzene-*m*-xylene separation problems. Figures presented in Table 5 indicate that HDO is likely to be a good extraction solvent for the separation of heptane-pyridine, heptane-thiophene, heptane-propan-2-none, hexane-methanol, octane-acetonitrile and octane-ethyl acetate pairs as its performance compares well with that of other listed solvents. $S_{ij}^{\infty}$ and $k_j^{\infty}$ values associated with HDO for alkanes-pyridine and alkanes-thiophene separations were remarkably high. These separation problems are significant in extraction processes such as the denitrification and desulfurization of fuels in petrochemical and chemical industries. While, in some instances, HDO may not perform better than ionic liquids, DESs and other molecular solvents, it can still be considered as separation solvent for heptane-pyridine, heptane-thiophene, heptane-propan-

**Table 5**
Selectivity and capacity at infinite dilution of various solvents for common industrial separation problems at $T$ = 323.15 K.

| Solvent | Heptane/ pyridine | Heptane/ thiophene | Water/ butanol | Cyclohexane/ benzene | Hexane/ methanol | Octane/acetonitrile | Octane/ ethylacetate | Ethylbenzene/ *m*-xylene | Heptane/ 2-propanone | Reference |
|---|---|---|---|---|---|---|---|---|---|---|
| Hdiol | 326.7/12.2 | 64.91/2.18 | 1.08/0.72 | 2.63/0.2 | 24.07/1.11 | 9.86/0.25 | 78.60/2.0 | 1.02/0.11 | 5.57/0.26 | This study |
| DES 1; [$4C_1$NBr]+[Hdiol] [1:2] | 354.3/13 | 177.13/6.3 | – | 5.41/0.49 | 64.39/3.03 | – | 107.51/2.86 | – | – | [16] |
| DES 2; [$4C_1$NCl]+[Hdiol] [1:1] | – | 538/4.42[a] | – | 3.71/0.1 | 57.03/0.81 | – | 114.82/0.95 | – | – | [15] |
| DES 3; [ChCl]+[Gly] [1:1] | 378.1/4.56 | 101/0.22[a] | – | 8.57/0.04[b] | – | – | 18.6/0.04 | – | – | [18] |
| DES 4; [ChCl]+[Gly] [1:2] | – | 62.1/0.31[c] | – | 5.65/0.06[b] | – | – | 18.06/0.8 | – | – | [18] |
| DES 5; [$4C_1$NCl]+[EG] [1:2] | 3774/2.53 | 1389/0.93 | – | 1.93/0.05 | 2535/1.52 | – | – | – | – | [17] |
| DES 6; [$4C_1$NCl]+[Gly] [1:2] | – | 93.15/0.38 | – | 4.45/0.02 | 204.3/0.82 | – | 44.45/0.19 | – | – | [30] |
| [$N_{1,1,12,2OPh}$] [$NTf_2$] † | 10.2/3.44 | 5.44/1.83 | 2.58/0.74 | 3.48/1.71 | 2.73/0.93 | 8.51/2.08 | 7.89/1.93 | 1.06/1.14 | 7.49/2.51 | [43] |
| [ChxmPyrr] [$Tf_2$N] | 26.2/2.13 | 18.92/1.54 | 1.04/0.45 | 7.69/1.35 | 6.89/0.74 | 32.16/1.96 | 21.03/1.28 | 1.0/0.74 | 18.64/1.52 | [44] |
| [BzPy] [$Tf_2$N] | 51.3/2.13 | 33.01/1.37 | 1.21/0.41 | 10.11/1.10 | 13.66/0.81 | 82.62/2.38 | 47.53/1.37 | 1.01/0.55 | 36.52/1.52 | [44] |
| [*sec*-BMIm] [$Tf_2$N] | 40.3/1.8 | 24.03/1.06 | 1.21/0.41 | 8.94/0.93 | 13.42/0.83 | 66.13/2.08 | 38.71/1.22 | 1.01/0.45 | 29.72/1.32 | [45] |
| [BMPYR] [DCA] | 0.005/0.00 | 88.28/1.18 | – | 6.27/0.71 | – | 166.17/1.5 | 47.03/0.42 | 0.99/0.29 | 41.676/0.56 | [46] |
| [EMMor] [DCA] † | 386.8/0.56 | 298.7/0.44 | 0.11/0.33 | 35.24/0.22 | – | 913/1.01 | 155.5/0.17 | 1.09/0.07 | 127.2/0.19 | [47] |
| [$N_{2,2,2,8}$] [FSI] † | 25.56/2.25 | 20.12/1.77 | 1.93/0.41 | 8.05/1.53 | 5.41/0.61 | 26.72/1.84 | 15.70/1.08 | 1.05/0.87 | 16.57/1.46 | [48] |
| [*N*-$C_3$OHMIM] [DCA] † | 309.7/0.73 | 169.5/0.4 | 0.13/0.36 | 21.07/0.22 | 428/1.58 | 131.35/0.2 | 113.45/0.17 | 1.03/0.07 | 84.23/0.2 | [49] |
| [$P_{8,8,8,8}$] [$NTf_2$] † | 4.05/2.87 | 3.3/2.34 | 6.12/0.76 | 2.07/2.34 | 0.87/0.72 | 2.84/1.77 | 3.4/2.12 | 1.02/1.63 | 4.27/3.03 | [50] |
| [AMIM] [DCA] † | 170.0/0.81 | 114.2/0.55 | 0.19/0.56 | 100.9/2.0 | 260/2.0 | 361.51.08 | 87.65/0.26 | 1.02/0.11 | 64.61/0.31 | [51] |
| [*N*-$C_3$OHPY] [DCA] † | 321.25/0.7 | 173.6/0.38 | – | 20.08/0.2 | 411.2/1.46 | 584.4/0.79 | 114.3/0.15 | 0.22/0.07 | 173.6/0.38 | [52] |
| Sulfolane† | 45.71/0.90 | 45.62/0.9[d] | 1.66/0.41 | 8.0/0.43 | 18.8/0.51 | 47.2/0.93[e] | 19.6/0.40[f] | – | – | [53] |
| NMP | – | – | – | 6.5/0.97 | – | – | – | – | 2.07/0.57[g] | [40] |

† Intepolated values.
[a] octane/pyridine.
[b] $T$ = 313.15 K.
[c] $T$ = 333.15 K.
[d] heptane/pyridine.
[e] heptane/acetonitrile.
[f] heptane/ethylacetate.
[g] heptane/2-butanone; [$4C_1$NBr] + [Hdiol]: tetramethylammonium bromide + 1,6 hexanediol; [$4C_1$NCl] + [Hdiol]: tetramethylammonium chloride + 1,6 hexanediol; [ChCl] + [Gly]: choline chloride + glycerol; [$4C_1$NCl] + [EG]: tetramethylammonium chloride + ethylene glycol; [$4C_1$NCl] + [Gly]: tetramethylammonium chloride + glycerol; [BMPYR][DCA]: 1-butyl-1-methylpyrrolidynium dicyanamide; [$N_{1,1,12,2OPh}$][NTf2]: dimethyldodecylphenoxyethylammonium bis{(trifluoromethyl)sulfonyl}; [$N_{2,2,2,8}$][FSI]: *N*-triethyl-*N*-octylammonium bis(fluorosulfonyl)imide imide; [*N*-$C_3$OHPY][DCA]: 1-(3-hydroxypropyl)pyridinium dicyanamide; [EMMor][DCA]: *N*-ethyl-*N*-methylmorpholinium dicyanamide; [*N*-$C_3$OHMIM][DCA]: 1-(3-hydroxypropyl)-3-methylimidazolium dicyanamide; [*sec*-BMIm][$Tf_2$N]: 1-*sec*-butyl-3-methylimidazolium bis(trifluoromethylsulfonyl)imide; [AMIM][DCA]: 1-allyl-3-methylimidazolium dicyanamide; [$P_{8,8,8,8}$][$NTf_2$]: tetraoctylphosphonium bis{(trifluomethyl)sulfonyl} imide; [ChxmPyrr][$Tf_2$N]: 1-cyclohexylmethyl-1-methylpyrrolidinium bis(trifluoromethylsulfonyl)imide; [BzPy][$Tf_2$N]: 1-benzylpyridinium bis(trifluoromethylsulfonyl)imide.

**Table 6**
Comparison of infinite dilution activity coefficients for selected organic solutes at 323.15 K.

| Solvent | n-Hexane | Cyclohexane | Hex-1-ene | Ethanol | Benzene | Acetone | Thiophene | Pyridine | Methyl acetate | Ref |
|---|---|---|---|---|---|---|---|---|---|---|
| Hdiol | 21.7 | 15.4 | 15.4 | 1.1 | 5.1 | 2.7 | 0.5 | 0.1 | 0.5 | This study |
| DES 1; [$4C_1$NBr] + [Hdiol] [1:2] | 21.3 | 11.0 | 13.3 | 0.5 | 2.0 | 1.6 | 0.2 | 0.1 | 0.3 | [16] |
| DES 2; [$4C_1$NCl] + [Hdiol] [1:1] | 70.5 | 35.6 | 52.6 | 1.7 | 9.7 | 4.9 | 0.8 | 0.2 | 1.0 | [15] |

2-none, hexane-methanol, octane-acetonitrile and octane-ethyl acetate pairs, on the basis of its low cost and low toxicity.

### 4.4. Comparison between HDO and HDO-containing DESs

Table 6 presents a comparison of experimental $\gamma_{13}^{\infty}$data between tetramethylammonium chloride + 1,6 hexanediol deep eutectic solvent in the 1:1 M ratio (DES1) [15] as well as tetrapropylammonium bromide + 1,6-hexanediol deep eutectic solvent in the 1:1 M ratio (DES2) [16] with pure HDO at $T$ = 323.15 K. All previously investigated solute groups are represented in this table. It can be observed that DES2 have higher values of activity coefficients at infinite dilution followed by pure HBO and finally DES1. The two hydroxyl groups of HDO interact strongly with the positive sites of solutes. This results into strong dipole-dipole interactions or hydrogen bonds. The presence of hydrogen bond acceptors in DES 1 and DES 2 lead to increased solvent-solvent interactions (hydrogen bonds) which competed with solute-solvent interactions. In other words, solute-solvent interaction were weaken by the presence of strong hydrogen bonds between the molecules comprising the two deep eutectic solvents. As expected, the weakest solvent-solvent interactions (expected in DES1) corresponded to the strongest solvent-solute interactions, i.e. to the lowest limiting activity coefficients observed in DES2.

As part of this study, a comparison was made between DES1, DES2 and HDO in terms of their separation performance (See Table 5). It emerged that forming DESs with appropriate hydrogen bond acceptors such as ammonium-based salts can enhance HDO separation performance. This was indicated by selectivity values related to HDO being generally lower than those obtained for HDO-containing DESs.

## 5. Conclusion

The GLC technique has been used to measure $\gamma_{13}^{\infty}$ for a series of 35 polar, and nonpolar organic solutes in the temperature range from (323.15 to 353.15) K. Experimental $\gamma_{13}^{\infty}$ data allowed the determination of partition coefficients between HDO and helium, as well as, excess molar Gibbs free energy, molar entropy and excess molar enthalpy values at infinite dilution. The following five-point conclusion can be drawn:

- HDO interacts more strongly with polar solutes than non-polar solutes,
- Mixing in HDO-containing systems is spontaneous in the case of highly polar molecules,
- Solutes interact more strongly with HDO than HDO-containing deep eutectic solvents,
- HDO is likely to serve as effective solvent in fuel denitrification and desulfurisation processes,
- Combining HDO with hydrogen acceptors leads to better separation performance for various mixtures.

The finding of this study allowed to understand the role played by hydrogen bond acceptors (HBA) in defining the separation performance of HDO-containing deep eutectic solvents. Furthermore, the data reported herin can be used to develop or refine thermodynamic models to describe systems involving HDO.

## CRediT authorship contribution statement

**Nkululeko Nkosi:** Methodology, Investigation, Writing - original draft. **Kaniki Tumba:** Conceptualization, Supervision, Project administration, Conceptualization, Data curation, Writing - review & editing. **Peterson Ngema:** Resources, Writing - review & editing. **Suresh Ramsuroop:** Supervision, Writing - review & editing.

## Declaration of Competing Interest

The authors declare that they have no known competing financial interests or personal relationships that could have appeared to influence the work reported in this paper.

## Acknowledgements

This study has been supported by the Durban University of Technology and Mangosuthu University of Technology. Author N. Nkosi wishes to thank the Council for Scientific and Industrial Research (CSIR) in South Africa for the financial support while undertaking this research project.

## Appendix A. Supplementary data

Supplementary data to this article can be found online at https://doi.org/10.1016/j.jct.2020.106163.

## References

[1] Ullmann's Encyclopedia of Industrial Chemistry: Sixth, Completely Revised Edition. Volumes 1–40 Edited by Wiley-VCH. Wiley-VCH: Weinheim, 2003, 30000 pp.
[2] Y. Takeda, M. Tamura, Y. Nakagawa, K. Okumura, K. Tomishige, Hydrogenation of dicarboxylic acids to diols over Re-Pd catalysts, Catal. Sci. Technol. 6 (2016) 5668–5683, https://doi.org/10.1039/c6cy00335d.
[3] R. Jaganathan, S.T. Chaudhari, C.V. Rode, R.V. Chaudhari, P.L. Mills, Hydrogenation of diethyl adipate in a catalytic fixed-bed reactor, Ind. Eng. Chem. Res. 37 (1998) 2099–2106, https://doi.org/10.1021/ie970631a.
[4] P. Regina, D. Irina, Efficient utilization of renewable feedstocks: the role of catalysis and process design, Philos. Trans. R. Soc. A Math. Phys. Eng. Sci. 376 (2018) 20170064, https://doi.org/10.1098/rsta.2017.0064.
[5] F.C.A. Figueiredo, E. Jordão, W.A. Carvalho, Adipic ester hydrogenation catalyzed by platinum supported in alumina, titania and pillared clays, Appl. Catal. A Gen. 351 (2008) 259–266, https://doi.org/10.1016/j.apcata.2008.09.027.
[6] J. Zhang, H. Li, X. Ma, H. Li, S. Yang, L. Xu, G. Liu, Solubility and thermodynamics of mixing of 1,6-Hexanediol in ethyl acetate + (methanol or n-butanol) at various temperatures, J. Mol. Liq. 242 (2017) 868–872, https://doi.org/10.1016/j.molliq.2017.07.095.
[7] K.A.E. Stenberg, M. Vihinen, Crystal structure of a 1.6-hexanediol bound tetrameric form of Escherichia coli lac-repressor refined to 2.1 Å resolution, Proteins Struct. Funct. Bioinforma. 75 (2009) 748–759, https://doi.org/10.1002/prot.22284.
[8] J. Zhang, S. Yang, H. Li, P. Yu, L. Xu, G. Liu, Solubility and thermodynamic analysis of 1,6-Hexanediol in (methanol + dimethyl adipate) and (n-butanol + dimethyl adipate) binary solvents from 283.15 K to 303.15 K, J. Mol. Liq. 238 (2017) 310–315, https://doi.org/10.1016/j.molliq.2017.03.119.
[9] X. Yang, H. Li, C. Cao, L. Xu, G. Liu, Experimental and correlated liquid-liquid equilibrium data for dimethyl adipate + 1,6-hexanediol + water or ethylene glycol, J. Mol. Liq. 284 (2019) 39–44, https://doi.org/10.1016/j.molliq.2019.03.115.

[10] C.M. Romero, M.S. Páez, J.A. Miranda, D.J. Hernández, L.E. Oviedo, Effect of temperature on the surface tension of diluted aqueous solutions of 1,2-hexanediol, 1,5-hexanediol, 1,6-hexanediol and 2,5-hexanediol, Fluid Phase Equilib. 258 (2007) 67–72, https://doi.org/10.1016/j.fluid.2007.05.029.
[11] Z.S. Lin, Y. Huang, Tetraalkylammonium salt/alcohol mixtures as deep eutectic solvents for syntheses of high-silica zeolites, Microporous Mesoporous Mater. 224 (2016) 75–83, https://doi.org/10.1016/j.micromeso.2015.11.008.
[12] H.E. Park, B. Tang, K.H. Row, Application of Deep Eutectic Solvents as Additives in Ultrasonic Extraction of Two Phenolic Acids from Herba Artemisiae Scopariae, Anal. Lett. 47 (2014) 1476–1484, https://doi.org/10.1080/00032719.2013.874016.
[13] D.E. Yoo, K.M. Jeong, S.Y. Han, E.M. Kim, Y. Jin, J. Lee, Deep eutectic solvent-based valorization of spent coffee grounds, Food Chem. 255 (2018) 357–364, https://doi.org/10.1016/j.foodchem.2018.02.096.
[14] Q. Cui, X. Peng, X.H. Yao, Z.F. Wei, M. Luo, W. Wang, C.J. Zhao, Y.J. Fu, Y.G. Zu, Deep eutectic solvent-based microwave-assisted extraction of genistin, genistein and apigenin from pigeon pea roots, Sep. Purif. Technol. 150 (2015) 63–72, https://doi.org/10.1016/j.seppur.2015.06.026.
[15] N. Nkosi, K. Tumba, S. Ramsuroop, Activity coefficients at infinite dilution of various organic solutes in the deep eutectic solvent (tetramethylammonium chloride + 1,6 hexanediol in the 1:1 molar ratio), South African J. Chem. Eng. 27 (2019) 7–15, https://doi.org/10.1016/j.sajce.2018.11.003.
[16] N. Nkosi, K. Tumba, S. Ramsuroop, Activity coefficients at infinite dilution of various solutes in tetrapropylammonium bromide + 1,6-hexanediol deep eutectic solvent, J. Chem. Eng. Data. 63 (2018), https://doi.org/10.1021/acs.jced.8b00600.
[17] N. Nkosi, K. Tumba, S. Ramsuroop, Measurements of activity coefficient at infinite dilution for organic solutes in tetramethylammonium chloride + ethylene glycol deep eutectic solvent using gas-liquid chromatography, Fluid Phase Equilib. 462 (2018) 31–37, https://doi.org/10.1016/j.fluid.2018.01.019.
[18] S.P. Verevkin, A.Y. Sazonova, A.K. Frolkova, D.H. Zaitsau, I.V. Prikhodko, C. Held, Separation performance of biorenewable deep eutectic solvents, Ind. Eng. Chem. Res. 54 (2015) 3498–3504, https://doi.org/10.1021/acs.iecr.5b00357.
[19] M. Rogošić, K.Z. Kučan, Deep eutectic solvents based on choline chloride and ethylene glycol as media for extractive denitrification/desulfurization/dearomatization of motor fuels, J. Ind. Eng. Chem. 72 (2019) 87–99, https://doi.org/10.1016/j.jiec.2018.12.006.
[20] K.H. Almashjary, M. Khalid, S. Dharaskar, P. Jagadish, R. Walvekar, T.C.S.M. Gupta, Optimisation of extractive desulfurization using choline chloride-based deep eutectic solvents, Fuel 234 (2018) 1388–1400, https://doi.org/10.1016/j.fuel.2018.08.005.
[21] H. Malaeke, M.R. Housaindokht, H. Monhemi, M. Izadyar, Deep eutectic solvent as an efficient molecular liquid for lignin solubilization and wood delignification, J. Mol. Liq. 263 (2018) 193–199, https://doi.org/10.1016/j.molliq.2018.05.001.
[22] Q. Pan, X. Shang, J. Li, S. Ma, L. Li, L. Sun, Energy-efficient separation process and control scheme for extractive distillation of ethanol-water using deep eutectic solvent, Sep. Purif. Technol. 219 (2019) 113–126, https://doi.org/10.1016/j.seppur.2019.03.022.
[23] J.D. Raal, A.L. Muhlbauer, Phase Equilibria – Measurement and Computation, Taylor & Francis, 1997.
[24] K.A. Tumba, Infinite dilution activity coefficient measurements of organic solutes in fluorinated ionic liquids by gas-liquid chromatography and the inert gas, (2010), MSc Dissertation, University of KwaZulu-Natal, South Africa.
[25] T.M. Letcher, Activity coefficients at infinite dilution from gas–liquid chromatography, Faraday Symp. Chem. Soc. 15 (1980) 103–112, https://doi.org/10.1039/FS9801500103.
[26] P. Alessi, A. Alessandrini, M. Orlandini, Activity coefficients at infinite dilution in solvents with two functional groups, Chem. Eng. Commun. 27 (1984) 59–67, https://doi.org/10.1080/00986448408940491.
[27] M. Souto-Caride, J. Troncoso, J. Peleteiro, E. Carballo, L. Romaní, Viscosity anomaly near the critical point in nitrobenzene + alkane binary systems, Phys. Rev. E - Stat. Nonlinear, Soft Matter Phys. 71 (2005) 1–6, https://doi.org/10.1103/PhysRevE.71.041503.
[30] N. Nkosi, K. Tumba, S. Ramsuroop, Tetramethylammonium chloride + glycerol deep eutectic solvent as separation agent for organic liquid mixtures: assessment from experimental limiting activity coefficients, Fluid Phase Equilib. 473 (2018) 98–105, https://doi.org/10.1016/j.fluid.2018.06.003.
[31] I. Bahadur, B.B. Govender, K. Osman, M.D. Williams-Wynn, W.M. Nelson, P. Naidoo, D. Ramjugernath, Measurement of activity coefficients at infinite dilution of organic solutes in the ionic liquid 1-ethyl-3-methylimidazolium 2-(2-methoxyethoxy) ethylsulfate at T=(308.15, 313.15, 323.15 and 333.15)K using gas+liquid chromatography, J. Chem. Thermodyn. (2014) 245–252, https://doi.org/10.1016/j.jct.2013.10.017.
[32] D.H. Everett, Effect of gas imperfection on G.L.C. measurements: a refined method for determining activity coefficients and second virial coefficients, Trans. Faraday Soc. 61 (1965) 1637, https://doi.org/10.1039/tf9656101637.
[33] A.J.B. Cruickshank, B.W. Gainey, C.P. Hicks, T.M. Letcher, R.W. Moody, C.L. Young, Gas-liquid chromatographic determination of cross-term second virial coefficients using glycerol. Benzene + nitrogen and benzene + carbon dioxide at 50°C, Trans. Faraday Soc. 65 (1969) 1014–1031, https://doi.org/10.1039/TF9696501014.
[34] B.E. Poling, J.M. Prausnitz, J.P. O'Connel, The properties of gases & liquids, 2001. doi:10.1016/0894-1777(88)90021-0.
[35] D.R. Lide, CRC Handbook of Chemistry and Physics, 84th Edition, 2003-2004, Handb. Chem. Phys. (2003). doi:10.1136/oem.53.7.504.
[36] M. McGlashan, D. Potter, An apparatus for the measurement of the second virial coefficients of vapours; the second virial coefficients of some n-alkanes and some mixtures of n-alkanes, Proc. R. Soc. London A 267 (1962) 478–500, https://doi.org/10.1098/rspa.1962.0114.
[37] G.H. Hudson, J.C. McCoubrey, Intermolecular forces between unlike molecules. A more complete form of the combining rules, Trans. Faraday Soc. 56 (1960) 761, https://doi.org/10.1039/tf9605600761.
[38] C. Tsonopoulos, J.H. Dymond, A.M. Szafranski, Second virial coefficients of normal alkanes, linear 1-alkanols and their binaries, Pure Appl. Chem. 61 (1989) 1387–1394, https://doi.org/10.1351/pac198961081387.
[39] J.M. Smith, H.C. Van Ness, M.M. Abbot, Introduction to Chemical Engineering Thermodynamics, 2000.
[40] M. Krummen, J. Gmehling, Measurement of activity coefficients at infinite dilution in N-methyl-2-pyrrolidone and N-formylmorpholine and their mixtures with water using the dilutor technique, Fluid Phase Equilib. 215 (2004) 283–294, https://doi.org/10.1016/j.fluid.2003.10.010.
[42] O. Odele, S. Macchietto, Computer-aided molecular design: a novel method for optimal solvent selection, Fluid Phase Equilib. (1993), https://doi.org/10.1016/0378-3812(93)87128-N.
[43] U. Domańska, M. Karpińska, A. Wiśniewska, Z. Dąbrowski, Ammonium ionic liquids in extraction of bio-butan-1-ol from water phase using activity coefficients at infinite dilution, Fluid Phase Equilib. 479 (2019) 9–16, https://doi.org/10.1016/j.fluid.2018.09.024.
[44] F. Mutelet, S. Ravula, G.A. Baker, D. Woods, X. Tong, W.E. Acree, Infinite dilution activity coefficients and gas-to-liquid partition coefficients of organic solutes dissolved in 1-benzylpyridinium bis(trifluoromethylsulfonyl)imide and 1-cyclohexylmethyl-1-methylpyrrolidinium bis(trifluoromethylsulfonyl) imide, J. Solution Chem. 47 (2018) 308–335, https://doi.org/10.1007/s10953-018-0720-5.
[45] F. Mutelet, G.A. Baker, S. Ravula, E. Qian, L. Wang, W.E. Acree, Infinite dilution activity coefficients and gas-to-liquid partition coefficients of organic solutes dissolved in 1-sec-butyl-3-methylimidazolium bis(trifluoromethylsulfonyl) imide and in 1-tert-butyl-3-methylimidazolium bis(trifluoromethylsulfonyl) imide, Phys. Chem. Liq. 00 (2018) 1–20, https://doi.org/10.1080/00319104.2018.1491045.
[46] M. Durski, P. Naidoo, D. Ramjugernath, U. Domańska, Thermodynamics and activity coefficients at infinite dilution for organic solutes in the ionic liquid 1-butyl-1-methylpyrrolidinium dicyanamide, Fluid Phase Equilib. 473 (2018) 175–182, https://doi.org/10.1016/j.fluid.2018.06.013.
[47] U. Domańska, M. Karpińska, M. Wlazło, Thermodynamic study of molecular interaction-selectivity in separation processes based on limiting activity coefficients, J. Chem. Thermodyn. 121 (2018) 112–120, https://doi.org/10.1016/j.jct.2018.02.014.
[48] U. Domańska, M. Karpińska, The use of ionic liquids for separation of binary hydrocarbons mixtures based on gamma infinity data measurements, J. Chem. Thermodyn. 127 (2018) 95–105, https://doi.org/10.1016/j.jct.2018.07.024.
[49] M. Karpińska, M. Wlazło, M. Zawadzki, U. Domańska, Separation of binary mixtures hexane/hex-1-ene, cyclohexane/cyclohexene and ethylbenzene/styrene based on gamma infinity data measurements, J. Chem. Thermodyn. 118 (2018) 244–254, https://doi.org/10.1016/j.jct.2017.11.017.
[50] U. Domańska, M. Wlazło, M. Karpińska, M. Zawadzki, High selective water/butan-1-ol separation on investigation of limiting activity coefficients with [P8,8,8,8][NTf2] ionic liquid, Fluid Phase Equilib. 449 (2017) 1–9, https://doi.org/10.1016/j.fluid.2017.06.001.
[51] M. Wlazło, J. Gawkowska, U. Domańska, Separation based on limiting activity coefficients of various solutes in 1-allyl-3-methylimidazolium dicyanamide ionic liquid, Ind. Eng. Chem. Res. 55 (2016) 5054–5062, https://doi.org/10.1021/acs.iecr.6b00942.
[52] U. Domańska, M. Wlazło, M. Karpińska, M. Zawadzki, Separation of binary mixtures hexane/hex-1-ene, cyclohexane/cyclohexene and ethylbenzene/styrene based on limiting activity coefficients, J. Chem. Thermodyn. 110 (2017) 227–236, https://doi.org/10.1016/j.jct.2017.03.004.
[53] C. Möllmann, J. Gmehling, Measurement of Activity Coefficients at Infinite Dilution Using Gas−Liquid Chromatography. 5. Results for N -Methylacetamide, N, N -Dimethylacetamide, N, N -Dibutylformamide, and Sulfolane as Stationary Phases, J. Chem. Eng. Data. 42 (1997) 35–40. doi:10.1021/je9602226.

## *Further reading*

[28] J.G. Bleazard, T.F. Sun, R.D. Johnson, R.M. DiGuilio, A.S. Teja, The transport properties of seven alkanediols, Fluid Phase Equilib. 117 (1996) 386–393, https://doi.org/10.1016/0378-3812(95)02976-1.
[29] T. Lech, G. Czechowski, J. Jadzyn, Viscosity of the series of 1, n-alkanediols, J. Chem. Eng. Data. 46 (2001) 725–727, https://doi.org/10.1021/je0003750.
[41] B. Kolbe, J. Gmehling, Thermodynamic properties of ethanol + water. I. Vapour-liquid equilibria measurements from 90 to 150°C by the static method, Fluid Phase Equilib. 23 (1985) 213–226, https://doi.org/10.1016/0378-3812(85)90007-X.